

## Thermal Degradation of Poly(arylether sulfones)

### 2. Monte Carlo Simulation of Polymer Structure, Reaction, and Diffusion

C. Libanati, C. LaMarca, M. T. Klein\*, S. M. Andrews<sup>1</sup>,  
and R. J. Cotter<sup>1</sup>

Center for Catalytic Science and Technology  
Department of Chemical Engineering  
University of Delaware  
Newark, DE 19716

**keywords:** polymer, pyrolysis, modelling

#### INTRODUCTION

Sulfone-containing polyarylethers generally include one or more aromatic rings linked together by ether and sulfone groups. One class of these polymers also contains isopropylidene linkages. They form a class of polymers that are tough, have a high softening temperature, and maintain their desirable properties for extended periods of time.

The neat poly(arylether sulfones) are softened by heating for processing. The literature [38] suggests that some of the challenges to this processing are engendered by the valuable properties of the polymers themselves. The same desirable high temperature softening point for end-use applications is also high enough that some thermal degradation can occur during front-end processing. This can lead to gas evolution and viscosity increase, the latter presumably owing to the formation of a gel.

These literature reports motivated the present work aimed at applying our previously developed reaction modelling technique using Monte Carlo simulation to the reactions of poly(arylether sulfones). The particular appeal was that the literature suggested the thermal reactions have structural implications (e.g., gel formation), and our Monte Carlo technique is structurally explicit. There thus appeared to be a good match.

Our model therefore sought an explicit link among polymer structure, reactivity and properties. The link between polymer structure and reactivity was formed by basing the reaction pathways and kinetics on model compound chemistry. Part 1 of this series described the elementary steps modelled to control the thermal degradation of poly(arylether sulfones). The link between the thus-changing polymer structure and properties was established by phrasing the model in terms of a three-dimensional lattice, on which lattice sites represented monomer units and lattice site connections represented bonds. Polymer diffusion on this lattice was described by the movement of monomers to adjacent empty lattice sites. Polymer reaction was described by the destruction or formation of bonds between lattice sites, the nature and probabilities of which being described by model compound pathways and kinetics.

This percolation model of gelation allowed determination of gel, sol and gas fractions as a function of reaction time. Other relationships or models linking properties of the material to its structure (e.g., viscosity from molecular weight distribution or modulus from number of crosslinks and degree of polymerization between crosslinks) can be used to determine the adequacy of the polymer to the application for which it is intended.

The input to the model consists of the chemical and physical structure of the polymer of interest, an assumed mechanism of segmental mobility and associated transport constants, and the postulated mechanism of thermal reaction and its associated rate constants. The output is a prediction of the structure and chemical identity of the system as a function of time. Because the model describes the system at the molecular level, at which all polymers share structure and chemistry, the simulation parameters, such as reaction and transport time constants, are independent of the system modelled, and can be determined from other sources such as experiments with model compounds. Thus this model is envisioned as a tool for the understanding of the underlying fundamentals and for the determination and design of optimal systems.

Although models have been frequently used to improve qualitative understanding, any significant quantitative use of a model's prediction is achieved through comparison with laboratory experimental results. However, the lack of precise characterization of the starting material renders difficult quantitative comparisons between experimental studies and simulation results, especially when the polymers studied were synthesized for a particular study. In particular, a frequent omission in the studies reported in the literature is the molecular weight distribution of the original polymers studied. For the purpose of obtaining pertinent experimental data, we have developed our own experimental procedure which will be reported upon in a follow-up paper. Herein we focus on only the development and operation of the Monte

<sup>1</sup> Amoco Performance Products, Inc., 4500 McGinnis Ferry Rd., Alpharetta, GA 30202-3944.

Carlo simulation of polymer degradation. We begin by considering the basic issue of gelation, which controls the present structure-property link sought.

## GELATION AND PERCOLATION.

Part I described the basic chemistry of poly(arylether sulfone) degradation. Occurring in the polymer, these elementary steps have structural significance. We need to account for more than just the net bond formation/bond breaking; we need to account for crosslinking and longer-range connectivity. This requires a model of the gelation process. Gelation involves the formation of indefinitely large polymer structure, which will extend through the volume of the polymer sample and, on the molecular scale, may be considered essentially infinite.

Gelation is always the result of crosslinking. Its main characteristic is the existence of a gelation point or threshold. This point is akin to the critical point in thermodynamics. As conversion increases during the polymerization of a system containing multi-functional monomers, a point is reached where the system suddenly changes from a viscous homogeneous fluid to a two-phase system, containing an insoluble cluster, the gel, and a soluble portion, the sol [1-8,11, 12,20]. The existence of a gelation point has also been demonstrated in systems where initial constituents are not monomers but linear polymers [1,9-16].

Models of gelation address the connectivity of the system. An early analytical model was developed by Flory and Stockmayer [1,11,12]. Their approach is based on three main assumptions: functional groups react independently of one another; identical functional groups have the same reactivity; no intramolecular reactions occur. Also, any functional group can react with any other functional group, independent of position, and excluded volume effects are neglected.

Based on these assumptions, the system can be represented as a Bethe lattice [5] of functionality equal to the functionality of the monomers. A statistical analysis on this network provides information on the size of the clusters and the connectivity of the monomers as a function of conversion,  $p$  being defined as the number of bonds formed over the total number of possible bonds. This approach correctly describes the gelation transition and the critical conversion value  $p_c$  for the existence of an infinite cluster, calculated as  $p_c = 1/(f-1)$ , for monomer of functionality  $f$  [1]. The same approach has also been used to describe the crosslinking of linear polymer chains in the vulcanization of rubber [9,10,13-16].

The assumptions stated earlier limit the quantitative use of the analytical approach to but a handful of simple systems. For instance, neglecting intramolecular reaction is probably unreasonable when the initial condition is a set of large linear molecules rather than a collection of monomers. Also, excluded volume effects become important as the reaction proceeds, generating isolated sites, and the equal accessibility rule breaks down in strongly transport-limited systems. Percolation models of gelation are considered to account for the deficiencies of the analytical approach.

The central concept in percolation is the discrete description of space. Space is spanned by a lattice of dimensionality  $N$ . The lattice sites can be occupied by monomers, and are connected to neighboring sites by a certain number  $f$  of bonds, corresponding to the functionality of the monomers. It can be noted here that the Flory-Stockmayer approach is equivalent to a percolation of infinite dimensionality.

Percolation models are usually implemented numerically and grids of finite size are used to describe a representative fraction of the system. The boundaries of the grid are then considered to be periodic. In these instances, gelation is attained when percolation occurs. In other words, a cluster becomes infinite when it spans the length of the lattice. Based on the state of the lattice a slate of statistical quantities, regarding the composition of the system, can be calculated. The reaction network and kinetics determine the rules by which bonds are formed, linking  $p$  to reaction time.

In the case of poly(arylether sulfone) degradation, crosslinking occurs as a consequence of breaking and forming linkages within an initially linear polymeric system. The grid percolation models offer the advantage, over the analytical model, of describing the physical and chemical environment of a reactant. A reactive intermediate has a certain number of nearest neighbors with which it can react. Therefore, reactions can be considered at the elementary step level, where bond breaking and bond forming occur. These were presented in Part I and can be organized, from a topological point of view, into three main classes:

- |                           |   |
|---------------------------|---|
| Bond-breaking reactions:  | Initiations and eliminations from cyclohexadienyl, cyclohexyl or cyclohexenyl radicals. |
| Bond-forming reactions:   | Additions and terminations.   |
| "Bond-neutral" reactions: | Hydrogen abstractions and disproportionations.  |

In the next section, the Monte Carlo simulation of poly(arylether sulfone) degradation is presented, using a three-dimensional square-grid percolation model that incorporates the entire set of elementary steps described earlier.

## MONTE CARLO MODEL DEVELOPMENT.

The Monte Carlo simulation of degradation of poly(arylether sulfones) is summarized in terms of major modules of the overall simulation scheme. The initial polymer configuration is constructed from structural information. Once an original configuration is determined, radicals are generated within the grid using an event-space algorithm. The time  $t_i$  and nature of the initiating event (initiation reaction or diffusion into the lattice) are calculated. The new state of the system is determined, and time is updated (time = time +  $t_i$ ). Once radicals are present in the lattice, polymer segments are moved, and all radicals present are tested for reaction with their environment during a fixed time interval

$\Delta t$ . If, after that time interval, radicals are still present in the lattice, the total time is updated (time = time +  $\Delta t$ ), and the previous step is repeated. If, on the contrary, all radicals have disappeared from the lattice (via termination or by diffusing out through a grid boundary), new radicals are generated within the lattice. Then time is updated and the same movement/reaction process described above is repeated. Results are stored at desired reaction times. Once the final reaction time is reached, a new initial configuration is generated for each subsequent run. The results of all runs are averaged to yield statistically significant quantities.

The following subsections present in detail the features of each unit of the overall simulation, starting with the simulation of structure, including the initial configuration and the dynamic simulation of structure, followed by simulation of initiation and propagation reactions. The mechanics of the program developed are detailed elsewhere [39].

## SIMULATION OF STRUCTURE

The polymeric melt is represented by a three dimensional square grid of dimension  $N \times N \times N$ . Polymer chains are represented by monomers occupying grid sites connected by bonds. Each grid site has six nearest neighbors with which to interact through linkages or reaction. This representation of the system allows the description of the chemical environment of each site, as well as the global connectivity of the system. It also allows for spatial movement of the monomers, from site to site according to specified rules, to account for diffusion.

In poly(arylether sulfone) systems, the grid sites represent substituted benzene rings, and the bonds represent the linkages between aromatic units. For the system considered here, these bonds are sulfonyl linkages, ether linkages or carbon-carbon bonds (arising from thermal reaction).

### Initial configuration

The initial configuration of the system is determined by randomly placing molecules in the grid. Polymer molecules are initially linear. They are represented by self-avoiding random walks in the cubic lattice [1,20,17-19,21]. The degree of polymerization (chain length) of each molecule is randomly chosen from the initial degree of polymerization distribution. The molecule is then placed in the percolation grid, by placing monomers one by one, until the pre-determined length is attained. Where structure is concerned, the boundaries of the grid are periodic. This means that a polymer chain that exits the grid through one face reenters it through the opposite face. This procedure is repeated with new polymer chains until a fraction of the lattice, corresponding to the polymer's density, is filled.

In order to calculate the occupied fraction of the grid, the Van der Waals volume of the polymer, estimated by optimizing the structure of the polymer's building blocks (in this case diphenylsulfone and diphenyl ether), was compared with the total volume of the lattice, assumed to be the total volume occupied by the polymer. The estimation of the polymer molecular volume was achieved by optimizing structure using extended Hückel molecular orbital calculations. The occupied fraction was obtained by dividing the molar Van der Waals volume of the polymer's building block by the molar density of the polymer. In the case of poly(arylether sulfone), the density is 1.06 g/cc, and an average volume of diphenylsulfone and diphenylether was estimated at 130 Å<sup>3</sup>. The occupied fraction in this case is 75%.

The initial polymer configuration gives the complete connectivity of the polymeric melt, the free volume that will allow polymer movement and the chemical identity of each lattice site and bond. Reaction and movement of polymer units can then be explicitly addressed at the molecular level.

### Dynamic structure simulation.

The transport characteristics of the medium in which radical reactions occur have a strong influence on pathways and kinetics. The radical reactions involved in the degradation mechanism are very fast. Fast reactions have been shown to be affected by the ability of the reactant to move [22-24,28,30,32-36]. The time scale of these reactions is often comparable to that for molecular movement, especially in restricted systems like polymer melts. Also, the connectivity of the network can affect or be affected by transport limitations, as is apparent in the work of Brown in the radiolitic degradation of poly(arylether sulfone) at temperatures above and below the glass transition temperature [22]. It is therefore important to introduce mechanisms that account for the movement of the monomers.

The approach taken follows the idea that a polymer molecule diffuses through the movement of its smaller segments, in a wormlike fashion [39]. In simulation, a number of movements, equal to the number of monomers present in the medium, are attempted in a time step  $\Delta t$ . Since the CPU requirement to move every possible segment in the system becomes prohibitively large with grid size, only polymer segments within three lattice sites of a given radical were moved in one step. This local diffusion model captured the environment about a reactive site while still allowing reasonable computational demand. The model has been described in detail elsewhere [39].

### Simulation of Reaction

Reactions are simulated according to the stochastic algorithm described elsewhere [39]. Two classes of events are distinguished: The initiation events, creating active centers (radicals) within the lattice, and propagation events, carrying the radical chain reactions.

**Initiation Events.** Radicals responsible for the degradation of poly(arylether sulfone) are formed in initiation reactions. The sulfonyl linkages break to give two radicals, a phenyl radical and a sulfonyl radical. These radicals can propagate the reaction by interacting with stable monomers, or they can terminate.

An event-space algorithm is used to generate radicals. The initiation possibilities include the breaking of any of the  $N_{SO_2}$  sulfonyl linkages present in the lattice. Each one of them represents an event that can happen with rate constant  $k_{init}$ . However, due to the finite size of the grid, an extra initiation event was included: radicals generated elsewhere in the melt and outside of the lattice were allowed to diffuse into the grid. The necessity for such an event was prompted by the relative values of initiation and termination rate constants. Rate constants for initiation are usually orders of magnitude smaller than those for propagation reactions and up to  $10^{15}$  times smaller than termination rate constants. Concentrations of radicals in this system are of the order of  $10^{-8}$ – $10^{-10}$  times the concentration of initiating linkages. Memory availability and CPU requirement limit grid sizes to values well below the  $10^8$  sites necessary to simulate a representative sample of polymer melt. This means that periodic boundary conditions cannot be applied regarding the movement of radical intermediates. If a radical moves out of the percolation grid, it disappears. Having it reenter the grid through the opposing face would artificially increase the concentration of radicals. Including this second (transport) component to the "initiation" or generation of radicals involved the evaluation of the rate of "diffusion" of radicals into the lattice. This was accomplished by calculating the number of radicals that will cross the lattice boundaries inwards per unit time. A radical will move a distance equal to one lattice unit in an average time  $\tau = \pi l^2 / 16 D$ , where  $D$  is the effective diffusion coefficient and  $l$  is the size of a lattice unit. There are 6 neighboring sites to which the radical can move. If a radical is positioned one lattice site outside the lattice boundary, only one of its neighboring sites is part of the lattice. Thus, on average, 1/6 of the radicals in those positions will move into the lattice. The number of radicals diffusing into the lattice per unit time is then  $n_{rad} = C_{rad} \times V / 6 \tau$ , where  $C_{rad}$  is the global concentration of radicals in the melt and  $V = 6 (N l)^2$  is the volume represented by a slab one-lattice-site thick around the outside of the lattice boundaries. Estimations of  $C_{rad}$  and  $D$  were required in order to calculate  $n_{rad}$ .

The effective diffusion coefficient of radicals is a result of the combined effect of the mobility of polymer chains and segments and the reaction of radicals with occupied neighboring sites. The diffusing species is the radical reactive center and can move from molecule to molecule by reaction. This means that a radical center can "diffuse" even when the molecules bearing it are fixed.

The effective diffusion coefficient was therefore related not only to the physical characteristics of the system, through its transport properties (i.e. viscosity, molecular weight, crosslinks) but to its chemical structure as well. It was evaluated by placing a radical in the center of the reactive lattice and performing the simulation disabling initiation and termination chemistry. The average distance travelled,  $\bar{d}$ , by the radicals in a time  $t = 1$  second was recorded, and the diffusion coefficient was calculated by assuming the radical performed a random walk. In such a case,  $D = \pi \bar{d}^2 / 16 t$  or  $\bar{d}^2 / 6 t$ .

Finally, the evaluation of the rate of radicals diffusing into the lattice requires the knowledge of  $C_{rad}$ , the global concentration of radicals in the melt. The theory of reactions in solution as well as the pseudo-steady state approximation were applied to evaluate  $C_{rad}$  *a priori*, as described in detail elsewhere [39].

The final result is shown in Eq. 1, where  $[SO_2]$  is the concentration of unreacted  $SO_2$  linkages.

$$C_{rad} = \left( \frac{k_{init} k_d}{k_{term}} [-SO_2] \right)^{1/2} \quad (1)$$

The rate of diffusion of radicals into the lattice was thereby determined as a function of the physical and chemical characteristics of the real system and of the simulation parameters (i.e. grid size).

An event-space simulation is performed to calculate the time and nature of the next initiation event. The list of possible events includes the scission of any of the  $N_{SO_2}$  sulfonyl linkages and the diffusion of a radical into the lattice.

The total rate constant for radical generation is then  $k_{rg} = N_{SO_2} k_{init} + n_{rad}$ . The time interval between the present time and the next event,  $\tau$ , is determined according to the algorithm described elsewhere [36]. A random number, RN, is then drawn to determine which event occurred. If  $RN < N_{SO_2} k_{init} / k_{rg}$ , a sulfonyl linkage, chosen at random, breaks, generating two radicals. Otherwise, an occupied position selected at random on the lattice boundary is modified to become a radical (i.e. if the occupied position is a benzene ring, it is changed to a phenyl radical or a cyclohexadienyl radical, or to a phenoxy radical if it has phenoxy substituents), to represent the generation of an active center via diffusion. The reaction time was at this point updated by adding  $\tau$  to the current time.

Once reactive intermediates appeared in the lattice they could undergo a series of faster radical-molecule, radical-radical or  $\beta$ -scission reactions.

**Propagation reactions.** Propagation reactions can be strongly affected by segmental mobility. A fixed time step approach [37, 39] was used to simulate the reactions of radicals with their environment. A radical can react with any of its nearest neighbors to which it is not connected.

In the general case  $n$  reactions will be possible for a given radical. The probability for reaction  $i$  to occur is given by Equation (2):

$$P_i = \frac{k_i}{\sum_j k_j} \left( 1 - \exp \left( - \sum_j k_j \Delta t \right) \right) \quad (2)$$

The possible transitions and their associated probabilities are computed according to the environment of the radical and the energetics of elementary steps listed in Part 1. However, for bimolecular reactions, the reactants must come within one lattice unit of each other before they can react. Following the "reactions in solution" formalism, it is justified to say that they must form an encountered pair of reactant, A:B\*, for them to react. Chemical transformation of this pair is best described by a first-order process, the disappearance of the species identified as "an encountered pair of reactants". In short, the rate constants of Part 1 and the "reactions in solution" formalism [23,25,28] were reconciled

[39] to determine the transition probability for this first order process. The final result is  $k_{\text{first Order}} = \nu \rho \pi e^{-E^*/RT} = \frac{4}{3} \pi \rho^3 L A_{\text{second Order}} e^{-E^*/RT}$ , where the second order reaction and that of the encountered pair have the same activation energy.

To implement the simulation, the occurrence and nature of a reaction was determined through the algorithm for parallel reactions [37,39]. A random number,  $RN_i$ , was compared to the probability  $P_i = \left( 1 - \exp \left( - \sum_j k_j \Delta t \right) \right)$  that a radical  $i$  reacts. If reaction occurs a second random number determines its nature. The state of the lattice is then updated, and the random number  $RN_i$ , the rate constant of the reaction that did occur and  $\sum_j k_j$  are kept in memory. The same procedure is applied to all the radicals present in the lattice. The formalism of reactions in series [37,39] was used to account for the fact that several reactions in series can occur in  $\Delta t$ . If radical  $i$  reacts in the time interval to yield another radical (it does not terminate or "escape" from the grid), the new radical is tested for reaction. This procedure is repeated until no further reaction occurs.

Once all radicals have been checked for reaction in  $\Delta t$ , the reaction time is updated by adding  $\Delta t$  to the current time. A new time step is allowed to pass or new radicals are generated in the lattice depending on the status of the lattice. When the reaction time reaches predetermined output times, the status of the grid is recorded. Results of several Markov Chains are averaged to yield statistically significant numbers.

#### OUTPUT OF THE SIMULATION

The simulation results are recorded to allow for comparison with laboratory kinetics experiments. The computer "experiment" is the average of the results of  $N$  Markov Chains, for which results were recorded after 0-30 minutes of simulated reaction time.

The output of the simulation summarizes the detailed chemical structure and connectivity of the polymeric system as a function of reaction time. The attributes of the system are described in fractions (sol fraction, gel fraction, fraction of crosslinked monomers), averages (average molecular weight, average number of OH groups per monomer) or distributions (sol fraction molecular weight distribution, distribution of number of linkages per monomer).

The choice of attributes is often determined by the desired comparison with laboratory experiments, as is the case for the gel, sol and gas fractions. However, attributes unavailable from laboratory experiments may present considerable importance in the understanding of the underlying fundamentals. For example, the fraction of crosslinked monomers can be used to evaluate the validity of the Flory-Stockmayer model assumptions.

The quantities recorded for the present simulations were: distribution of monomer types (benzene rings, cyclohexadienes, cyclohexenes, cyclohexanes); total number of linkages; fraction of sulfonyl, ether and biphenyl linkages; fraction of monomers with one, two, three, and four linkages; gas, sol and gel fractions; number-average and weight-average molecular weight and degree of polymerization of the sol fraction; sol fraction molecular weight distribution; gas fraction composition; number of OH groups per monomer; number of chain ends; number of  $\text{SO}_2\text{H}$  groups per monomer; total number of radicals generated in the lattice.

Most of the foregoing quantities are determined by simple inspection of the lattice. Determination of gel, sol and gas fractions from the simulated pyrolysis requires more attention. Experimentally, these fractions are related to the solubility protocol used: the gas fraction is the portion of the mixture that is volatile at room temperature and one atmosphere total pressure; the gel fraction is the portion insoluble in a suitable solvent or any molecule unable to pass through a 5  $\mu$  micro-fiberglass filter; the sol fraction is the rest of material. The determination of the gel fraction was by making the conceptual link that the gel fraction corresponded to the portion of polymer that is insoluble in a solvent that dissolves linear polymers of same chemical compositions. The existence of a gel implies, according to Flory [1], the presence of an infinite network of crosslinked material.

#### SIMULATION RESULTS

Model predictions are presented in terms of temporal variation of average structural parameters and the yields of solubility-based product fractions from simulated poly(arylether sulfone) pyrolyses. The results presented here are the output of the simulation performed on a three-dimensional square grid of dimension 40 x 40 x 40.

## PRODUCT FRACTIONS

The determination of products belonging to the gel fraction, the sol fraction or the gas fraction was made according to the rules described above. Calculating the weight of each monomer and its associated linkages, summing these for the gel and sol fractions, and dividing by the total weight of all particles in these two fractions enabled prediction of the weight yield of the sol and gel fractions from simulated pyrolyses.

Figure 1 presents the temporal variations of the sol and gel product fractions for simulated pyrolysis at 425°C. The gel fraction shows a general increase with time, and the sol fraction shows the complementary decrease with time. A small fraction of gel is formed at times < 500 s, but a dramatic increase occurs at 500 s, where the gel fraction increases sharply to slightly greater than 20%. This can be qualitatively likened to the existence of a gelation point which has been reported during experimental polymer pyrolyses. The small fluctuations in the gel fraction prior to the dramatic increase can be attributed to computational factors. The simulation allows for bond-breaking initiations at all time steps. Chains already considered to be a part of the gel fraction can undergo chain scission at later reaction stages and therefore may no longer satisfy the percolation and crosslinking requirements for gelation. The frequency of this occurring is very small, however, and, in any event, dampens as the number of Markov Chains increases.

The yields of sulfur-containing product gases, H<sub>2</sub>S and SO<sub>2</sub>, from the simulated pyrolysis are shown in Figure 2. The percent yield is based on the amount of sulfone linkages contained in the reactant poly(arylether sulfone). The yield of SO<sub>2</sub> increases linearly with time and reaches an ultimate value of 4% after 1100 s of simulated reaction time. The percentage of H<sub>2</sub>S formed is much lower and achieves a value of only 0.1% after 1100 s of reaction time. The balance of the sulfur would remain in the gel or sol fraction as SO<sub>2</sub> linkages between monomers.

## STRUCTURAL PARAMETERS

The model explicitly monitored the length of each chain (number of monomeric units) and the type and number of links for each of the monomers. This information could be assembled to specify values of average structural parameters for the entire polymer or any of its product fractions.

The number average degree of polymerization,  $\bar{x}_n$ , for the sol product fraction as a function of time is presented in Figure 3. The value of  $\bar{x}_n$  is defined in the simulation as:

$$\bar{x}_n = \frac{\sum_i \text{number of chains of degree of polymerization } i \times i}{\text{total number of chains}}$$

where  $i=1$  would represent one unit in the polymer chain where a unit is taken to be a single benzene-derived ring or, in simulation terms, one grid point. Note that the value of  $\bar{x}_n$  continually decreases, exhibiting a value of 108 at the initial time and decreasing to an ultimate value of 20 at 1100 s. Chain scission and crosslinking have opposing effects on the value of  $\bar{x}_n$ . However,  $\bar{x}_n$  is particularly sensitive to the proportion, by number, of shorter chain lengths, and therefore exhibits the generally decreasing trend.

In the region of 500 s, there is a marked decrease in the value of  $\bar{x}_n$ . This is the point when a significant portion of gel fraction forms and the large, crosslinked chains no longer contribute to the value of  $\bar{x}_n$  for the sol fraction. The time at which this occurs is simultaneous with the point considered to be the gelation point in the gel fraction versus time curve presented above.

The temporal variation of the weight average degree of polymerization,  $\bar{x}_w$ , is shown in Figure 4. The definition of  $\bar{x}_w$  used in the simulation is:

$$\bar{x}_w = \frac{\sum_i \text{number of chains of degree of polymerization } i \times i^2}{\sum_i \text{number of chains of degree of polymerization } i \times i}$$

The value of  $\bar{x}_w$ , in contrast with the value of  $\bar{x}_n$ , increases with time in the initial stages of reaction. The weight average degree of polymerization is particularly sensitive to the presence of larger chain lengths, and therefore, the effect of crosslinking dominates over chain scission. The sharpest rise occurs in the region of 450 s followed by a sharp decline. This corresponds to the region, identified earlier as a gelation point. Here the infinite chains in the gel no longer contribute to any parameters measured in the sol fraction. In the later stages of reaction, more of the material is contained in the gel fractions, and the sol fraction is composed of small chains which gives rise to a small ultimate value of  $\bar{x}_w$ .

All of the results presented are for the reaction at 425°C of a poly(arylether sulfone) with a single initial degree of polymerization. We are just beginning to use the model to explore other polymers and conditions. The object of this report was to describe and record the approach and methodologies used. The agreement between model predictions and experimentally observed temporal variations of the yields of product fractions and the values of structural parameters will be assessed quantitatively in a follow-up communication.

## CONCLUSIONS

1. Poly(arylether sulfone) structure, reactions, and diffusion can be described quantitatively in terms of a dynamic reaction lattice.
2. Model compound kinetics provide a basis for modelling the bond-breaking and bond-forming reactions of poly(arylether sulfones).
3. Gelation was associated with the attainment of a spanning cluster on the lattice. The gel fraction was sensitive to the fraction of bonds formed, as in polymerization.
4. The model represents a flexible computer experiment for testing the influence of processing conditions.

## REFERENCES

1. Flory, P.S., *Principles of Polymer Chemistry*, Cornell University Press, Ithaca and London, 1953.
2. de Gennes, P. G., *Phys. Lett. A*, **38**, pp. 339-42, 1972.
3. de Gennes, P. G., *J. Physique*, **36**, pp. 1049-54, 1975.
4. Stauffer, D., *J. Chem. Soc. Faraday Trans II*, **72**, pp. 1354-64, 1976.
5. Stauffer, D., *Introduction to Percolation Theory*, Taylor and Francis, London and Philadelphia, 1985.
6. Coniglio, A., Starly, H. E., Klein, W., *Phys. Rev. Lett.*, **42**, pp. 518-22, 1979.
7. Earnoux, B., *Ann. Phys. Paris* **1**, pp. 73-141, 1976.
8. Lubensky, T. C. and Isaacson, S., *Phys. Rev. Lett.*, **41**, pp. 829-32, 1978.
9. Coniglio, A., Daout, M., *J. Phys. A: Meth. Gen.*, Vol. **12**, No. **10**, 1979.
10. Gonzalez, A.E., Daout, M., *J. Phys. A: Meth Gen*, **14**, pp. 2441-2457, 1981.
11. Stockmayer, W. H., *J. Chem. Phys.*, **11**, 45, 1943.
12. Stockmayer, W. H., *J. Chem. Phys.*, **12**, 125, 1944.
13. Gordon, M., *Proc. R. Soc. A.*, **268**, 240, 1962.
14. Gordon, M. and Malcolm, G. N., *Proc. R. Soc. A.*, **295**, 29, 1966.
15. Gordon, M. and Ross-Murphy, S. B., *Pure and Appl. Chem.* **43**, **1**, 1975.
16. Gordon, M. and Scontlelnry, G. R., *Proc. R. Soc.*, **292**, 380, 1966.
17. Weiss, G. H. and Rubin, R. J., "Random Walks: Theory and Applications," *Advances in Chemical Physics*, **52**, 1983.
18. Domb, C., *Adv. Chem. Phys.*, **15**, 229, 1969.
19. McKenzie, *Phys. Rep.*, **27C**, 35, 1976.
20. de Gennes, P. G., *Scaling Concepts in Polymer Physics*, Cornell University Press, Ithaca, N.Y., 1979.
21. Rudnick, J. and Graspari, G., *Science*, **237**, 1987.
22. Brown, J. R. and O'Donnell, J. H., "Effects of Gamma Radiation on Two Aromatic Polysulfones. II. A Comparison of Irradiation at Various Temperatures in Air-Vacuum Environments," *J. Appl. Polym. Sci.*, **23**, pp. 2763-2775, 1979.
23. Moore, J. W. and Pearson, R. G., *Kinetics and Mechanics*, John Wiley and Sons, New York, 1981.
24. Troe, J., *J. Phys. Chem.*, Vol. **90**, no. **30**, 1980.
25. Rabinowitch, E., *Trans Faraday Soc.*, **32**, 1381, 1936.
26. Fowler, R. H. and Slatev, N. B., *Trans Faraday Soc.*, **33**, 1185, 1937.
27. North, A. M., *The Collision Theory of Chemical Reactions in Liquids*, Methuen, London, 1964.
28. Smoluchowski, M. V., *Phys. Z.*, **17**, 1917.
29. Moelign-Hughes, E. A., *The Kinetics of Reactions in Solutions*, The Clarendon Press, Oxford, 2nd ed., 1947.
30. Noyes, R. M., *J. Am. Chem. Soc.*, **86**, 4529, 1964.
31. Noyes, R. M., *Prog. React. Kinet.*, **1**, 129, 1961.
32. Caldin, E. F. and Hasinoff, B. B., *J. Chem. Soc., Faraday Trans. I*, **71**, 515, 1975.
33. Trommsdorff, E., Kohle, H., Lagelly, P., *Makromolec. Chem.* **1**, 169, 1948.
34. Tulig, T. J. and Tinell, M., *Macromol.* **15**, 459, 1982.
35. Tulig, T. J. and Tinell, M., *Macromol.* **14**, 1501, 1981.
36. Rohr, D. and Klein, M. T., *I&EC Research*, **29**, 1210, 1990.
37. McDermott, J. B., Libanati, C., LaMarca, C. and Klein, M. T., *I&EC Research*, **29**, p. 22, 1990.
38. Rose, J. B., "Preparation and Properties of polyarylene ether sulphones," *Polymer* **15**, pp. 456-465, 1974.
39. Libanati, C., Ph.D. Thesis, University of Delaware, Newark, DE, 1990.

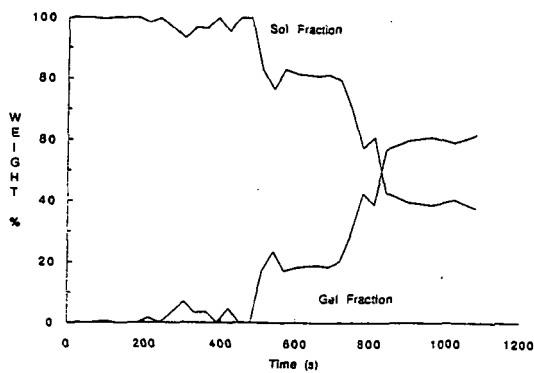


Figure 1. Temporal variation of gel and sol product fractions at 425°C from simulated poly(arylether sulfone) pyrolysis.

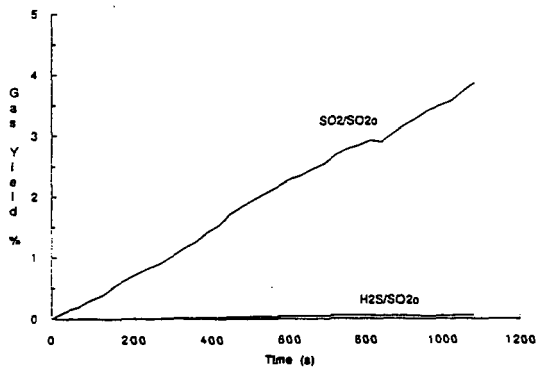


Figure 2. Temporal variation of sulfur-containing gas fraction at 425°C from simulated poly(arylether sulfone) pyrolysis.



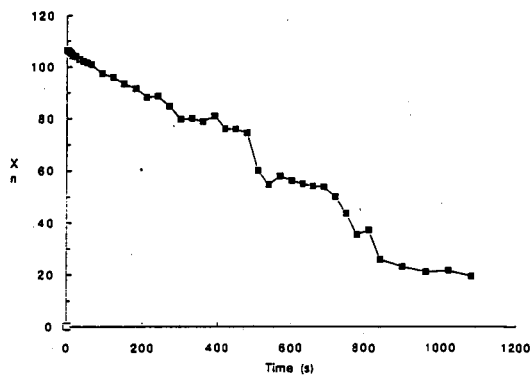


Figure 3. Temporal variation of number average degree of polymerization of sol fraction at 425°C from simulated poly(arylether sulfone) pyrolysis.

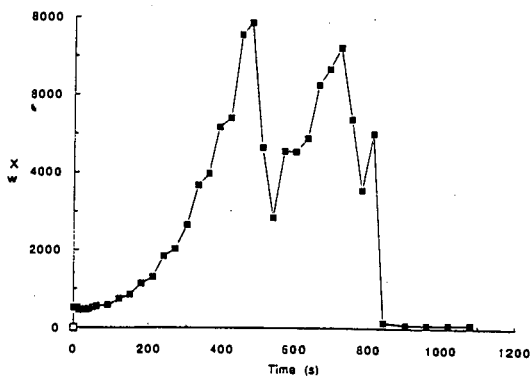


Figure 4. Temporal variation of weight average degree of polymerization of sol fraction at 425°C from simulated poly(arylether sulfone) pyrolysis.